Transactions of the Materials Research Society of Japan 29 [2] 425-428 (2004)

Stress depth profile in ceramic films on different interfacial layers

Shin Tsuchiya, Takatoshi Oshika*, Fumio Tsushima* and Akio Nishiyama*
Material Characterization Department, Central Research Institute, Mitsubishi Materials Corp.
1-297 Kitabukurocho, Omiya-ku, Saitama-shi, Saitama, Japan
Fax: 81-48-641-5998, e-mail: tsuchiya@mmc.co.jp
* Thin Film Materials Department, Central Research Institute, Mitsubishi Materials Corp.
1002-14 Mukohyama, Nakamachi, Naka-gun, Ibaraki, Japan
Fax: 81-29-295-5825, e-mail: oshika@mmc.co.jp, ftusima@mmc.co.jp, nishyam@mmc.co.jp

The residual stress near the interface between the films and the substrate degrades the adhesion strength of the films and therefore the life of the cutting tools. The origin of the residual stress is the difference in thermal expansion coefficients between the film and the substrate in case of CVD coated films. Consequently, relaxation of the thermal expansion coefficient mismatch at the interface leads to a reduction of the residual stress, i.e. an improvement of cutting performance of the tools. In this work, depth profiles of the residual stress in TiCN films coated on two different interfacial layers that have different thermal expansion coefficients were compared to examine a possibility of controlling the residual stress. A constant penetration depth method with synchrotron radiation available at SPring-8 was used to obtain the stress depth profiles. A difference in the stress depth profiles between the two TiCN films was observed though the method being under development. The TiCN film on the TiC layer showed lower residual stress than that of TiCN on TiN near the interface. The difference is ascribable to the fact that the thermal expansion coefficient of the TiC is between TiCN and WC-Co though that of TiN is larger than both TiCN and WC-Co.
Key words: residual stress, depth profile, adhesion, coating, penetration depth

1. INTRODUCTION

Ceramic coated cemented carbide tools are widely used for cutting, turning and milling operations. In these days the speed of such operations tends to be raised to improve an efficiency of machining processes. Hence the coated ceramic films become thicker to cope with the increase in the amount of wear. Thicker films, however, cause delamination because the adhesion strength is not enough to follow the plastic deformation of the cemented carbide substrate occurred in high speed operations. As the adhesion strength of the films is influenced by the residual stresses [1-4], it is important to know the residual stress especially near the interface.

In case of thin film, however, determining the residual stress is not easy because of preferred orientation and stress depth distribution. These two characteristics are often observed in thin films and make the application of the conventional $\sin^2\psi$ method difficult [5,6]. At the moment, there is no completely satisfactory stress measurement method for thin films that have both texture and stress depth distribution. In this work, a constant penetration depth method is adopted because the method doesn't need complicated calculations and relatively applicable to textured films.

One of the main components of the residual stress is a thermal stress resulted from the difference in the thermal expansion coefficients of the coating and the substrate [7]. For CVD coated films the thermal stress can be dominant [8]. Typical coating materials such as Al_2O_3, TiCN and TiN have been chosen in consideration of various aspects and can't be altered instantly. It means the reduction of the thermal stress is difficult if the coating temperature is set constant. On the other hand, thin interfacial layers are frequently used in CVD coating processes. Restrictions imposed on the interfacial layers are not so severe as wear resistant layers. Therefore the residual stress can be changed by an insertion of the interfacial layer which has an adequate thermal expansion coefficient.

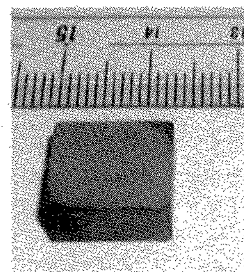

Fig.1 TiCN / (TiC or TiN) / WC-Co sample. 12.7mm square plane was measured

2. EXPERIMENT

2.1 Sample

CVD coated 10 microns thick TiCN layer was chosen as a target of the stress measurement. Two kinds of interfacial layers were separately deposited on cemented carbide substrates prior to the TiCN deposition. The thermal expansion coefficients of TiC and TiN interfacial layers are, 7.4 x 10^{-6} and 9.4 x 10^{-6} respectively. The former is smaller than the thermal expansion coefficient of

Fig.2 Structure and thermal expansion coefficients of each layer.

TiCN (8.4 x 10^{-6}) and larger than that of substrate (5.4 x 10^{-6}), the latter is larger than both TiCN and the substrate. Fig.1 and Fig.2 show a sample appearance and a schematic structure respectively.

A conventional θ/2θ diffractogram by Bragg-Brentano optics showed that the both TiCN films slightly have a preferred orientation toward (111) and (311) directions.

2.2 Stress measurement

As mentioned above the constant penetration depth method was used to measure the depth profiles of the residual stress in the films. X-ray penetration depth is different between iso-incline method and side-incline method even for the same ψ angle (Fig.3). It means that there is a region which gives a same penetration depth in

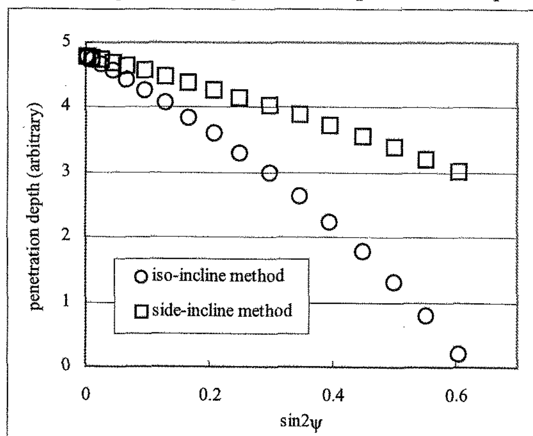

Fig.3 Comparison of the calculated penetration depth between the iso-incline and the side-incline method in conventional $\sin^2\psi$ method.

different ψ angles if iso-incline method and side-incline method are mixed.

The mixture is achieved by using the axes of ω and χ at the same time to set the ψ angle. ψ is defined as an angle between the sample surface normal and the diffracted lattice plane normal. Other angles such as ω or χ are defined as shown in Fig.4.

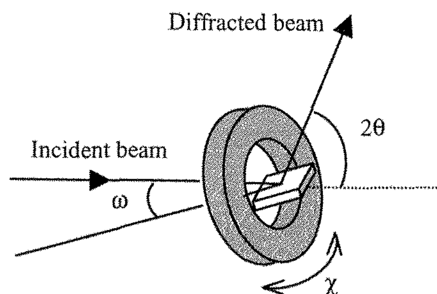

Fig.4 Definition of angles. Sample (white plate) is mounted on a χ circle (gray ring). The actual χ circle has a cut at the top (not shown).

An example of ω and χ angles is shown in Table I. These angles were calculated for TiCN (331) plane, photon energy of 8 KeV and penetration depth of 5.4 microns. In this condition, possible $\sin^2\psi$ range is restricted geometrically from 0.25 to 0.5. The sign of ω indicates the direction of tilting from the specular position. The negative sign means shallow (grazing) incidence and the positive is contrary.

The actual measurement was performed at the beam line BL19B2 in SPring-8 [9]. Measurement conditions are shown in Table II.

Table I. Example of ω and χ angles for TiCN (331) at 8KeV and penetration depth 5.4 microns.

	Actual angle		
$\sin^2\psi$	+ω	χ	−ω
0.200	82.809	inexecutable	21.172
0.225	82.066	inexecutable	21.915
0.250	81.249	83.057	22.732
0.275	80.344	75.363	23.637
0.300	79.335	70.374	24.646
0.325	78.197	66.307	25.783
0.350	76.902	62.740	27.079
0.375	75.407	59.488	28.574
0.400	73.647	56.452	30.334
0.425	71.522	53.570	32.459
0.450	68.853	50.800	35.128
0.475	65.248	48.108	38.733
0.500	59.300	45.471	44.681
0.525	inexecutable		
0.550	inexecutable		

Table II. Measurement conditions.

Sample	TiCN / TiC or TiN / WC-Co	
Measured plane	TiCN (331)	
Energy (KeV)	8	10
2θ (degree)	104	78
$\sin^2\psi$ range	0.2 to 0.7	0.2 to 0.8
Penetration depth (μm)	1.9, 3.4, 4.8, 6.7	5.5 to 14.4 (9 depths)
Omega mode	−ω (grazing incidence)	

X-ray irradiation area was controlled by an incident slit to be always smaller than the sample surface but was not kept constant. A soller slit with divergence angle 0.2 degree was placed just before a scintillation detector to improve the parallel beam optics. A sample spinner was used to average in-plane inhomogeneity of the sample and to increase the number of crystallites which contributed to the diffraction. The rotation speed of the spinner was ca. 360 degrees per minute. Both ω and χ axes were driven simultaneously during scans to keep the penetration depth as constant as possible.

3. RESULTS

3.1 Peak profile and $\sin^2\psi$ plot

Typical peak profiles are shown in Fig.5. At least 5000 counts at peak top were accumulated to minimize statistical error of counting. Any rough profile due to the statistical fluctuation or a large size crystallite was not observed. Peak position was determined by a curve fitting of Voigt function.

Fig. 6 shows peak position dependence on $\sin^2\psi$ for typical penetration depths of TiCN/TiN/WC measured at 8KeV (a) and 10KeV (b) respectively. A nonlinear behavior that appears when the conventional $\sin^2\psi$ method is applied to a sample with stress depth

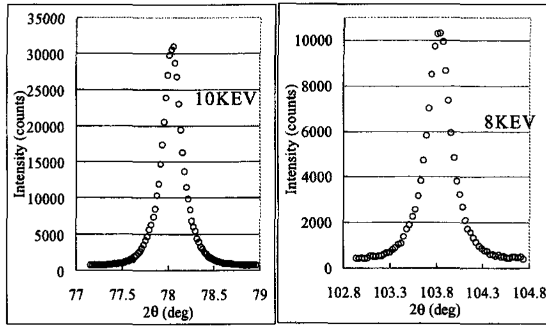

Fig.5 Typical peak profiles of TiCN (331) reflection taken by constant penetration depth method at 8KEV (right) and 10KeV (left).

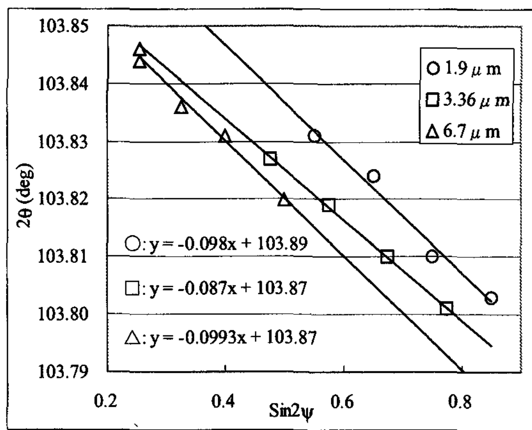

(a) 8KeV

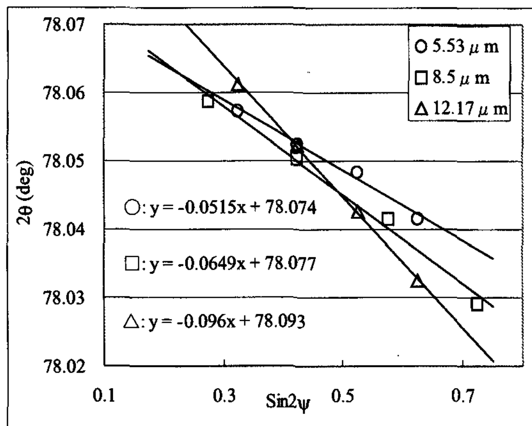

(b) 10KeV

Fig.6 $\sin^2\psi$ plot for TiCN (331) peak from TiCN/TiN/WC measured at 10KeV (a) and 8KeV (b). Only three depths are shown. The slope of linear fitting changed with the penetration depth.

distribution was not observed. This linearity also indicates that an effect of the preferred orientation was not significant. The slope of the linear fitting clearly changed with the penetration depth reflecting the stress depth distribution.

3.2 Stress depth profile

The stress distribution against the penetration depth is plotted in Fig.7. Yong's modulus 330GPa and Poisson's ratio 0.19 were used to calculate the stress from the slope of the $\sin^2\psi$ plots. Fitting curves shown in the plot have no theoretical background. They are chosen as the nearest approximation of the plot for a conversion described later.

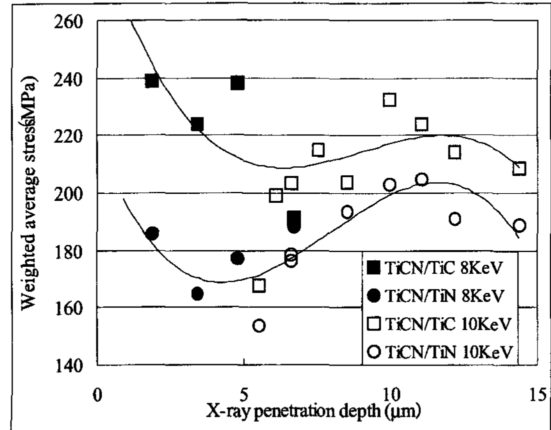

Fig.7 Stress depth profiles of TiCN on different interfacial layers. The vertical axis expresses the intensity weighted average stress. The horizontal axis is the penetration depth. Closed and open symbols correspond to data of 8KeV and 10KeV respectively. The doubly overlapped open circles are a result of reproducibility check.

The plotted data in Fig.7 didn't form smooth line. As the reproducibility of the measured stress value is estimated less than 5 MPa, the large data scattering in the depth profile probably has an origin that is not random but systematic nature.

As far as Fig.7 is referred, the stress of TiCN on TiC is larger than that of TiCN on TiN over the whole film thickness. This is because, however, the stress of TiCN on TiC near the surface is larger than TiCN on TiN. The large stress near the surface affects the measured stress in deeper region as the measured stress is weighted and averaged over the penetration depth.

The vertical axis of Fig.7 expresses the intensity weighted average stress and the horizontal axis is penetration depth. It is easier to understand the stress

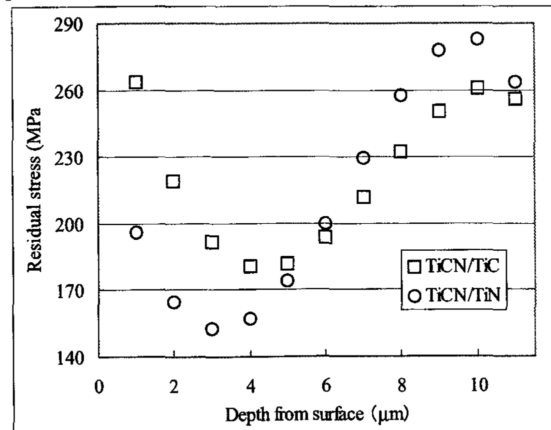

Fig.8 Stress depth profiles of TiCN derived from fitting curves in Fig.7. Vertical and horizontal axes were converted to residual stress and depth from sample surface respectively.

depth profile to have converted these axes to the residual stress and the depth from the sample surface. This conversion is known as the inverse Laplace transform [6]. The axes converted stress depth profile is shown in Fig.8.

The magnitude of the stress near the interface is reversed in Fig.8 compared with Fig.7. The stress of TiCN on TiC is lower than that of TiCN on TiN near the interface. On the other hand the stress of TiCN on TiC near the surface is still larger than that of TiCN on TiN.

The plot in Fig.8 is based on the fitting curves in Fig.7. The reliability of the fitting curves is not so high judging from the large data scattering in Fig.7. Consequently the reliability of Fig.8 is considered not to be so high especially from a quantitative view point.

4. DISCUSSIONS

4.1 Effect of interfacial layer

As noted in section 2.1, The thermal expansion coefficient of TiC interfacial layer is lower than the TiCN layer and is higher than the WC-Co substrate. On the other hand, the thermal expansion coefficient of TiN is larger than both TiCN and WC-Co. The extent of the mismatch is smaller in TiC system and this is considered to lead to the lower stress near the interface of TiCN/TiC. The thermal strain is smaller at TiC layer than TiN when cooled down to room temperature after the deposition. Therefore the adjacent TiCN region is not strained so much in TiC system comparing with TiN system. This results in the lower stress in TiC system near the interface. The above is though only a qualitative inference. A simulation or a direct measurement by some other method is needed for the confirmation and quantitative discussion.

4.2 Cause of data scattering

Fig.7 shows a large data scattering that probably is not random but systematic. There are several possibilities for the causes of the scattering. First of all, the stress may have an in-plane distribution in the radius direction, i.e. the stress can be different between the center and the near edge of the sample. In our measurement the sample was spun for the averaging in circumference direction but the irradiation area was not kept constant. The shape of the irradiation area was circular and its diameter varied from 4 to 10 mm depending on the scan. If there is inhomogeneity in the stress in the radius direction it would affect the measured value of the stress. Secondary, the optics adopted for the measurement was not perfect. For instance, the intensity of the incident X-ray has a distribution in horizontal direction. Though the incident slit width was set to be narrower than the limit where nonuniformity effect became detectable, a small possibility that the intensity distribution affects the peak position has been left. Thirdly, the possibility of the effect of the preferred orientation cannot be eliminated. The $\sin^2\psi$ plots didn't show a nonlinearity which is characteristic to a plot from textured sample. But even in the case of a $\sin^2\psi$ plot shows good linearity, the stress depth profile can exhibit a unreasonably complicated shape [10]. Unfortunately, however, how a preferred orientation affects to a diffracted peak position in the constant penetration depth measurement is not clearly understood. This is the problem which should be solved in future.

5. CONCLUSIONS

The stress depth distributions in TiCN films coated on either TiC or TiN interfacial layer were measured by constant penetration depth method using synchrotron radiation. The stress near the interface was lower in TiC system than in TiN system because of the medium thermal expansion coefficient of TiC.

A possibility of controlling residual stress near the interface by adjusting thermal expansion coefficient of thin interfacial layer was shown.

The constant penetration depth method was effective to obtain residual stress depth distributions in films though it needs to be improved as measured data has large scattering.

Acknowledgements

The authors wish to thank the staff of Japan Synchrotron Radiation Research Institute (JASRI) for their dedicated support in the stress measurements. A part of this work was entrusted by NEDO as "the Nanotechnology Program / the Nanostructure Coating Project" promoted by METI, Japan.

References

[1] H. K. Tönshoff and H. Seegers, *Surface and Coatings Technology*, **142-144**, 1100-1104, (2001).

[2] Y. Fu, H. Du, and C. Q. Sun, *Thin Solid Films*, **424**, 107-114, (2003).

[3] F. Vaz, L. Rebouta, Ph. Goudeau, J. P. Rivière, E. Schäffer, G. Kleer and M. Bodmann, *Thin Solid Films*, **402**, 195-202, (2002).

[4] Th. Göbel, S. Menzel, M. Hecker, W. Brückner, K. Wetzig and Ch. Genzel, *Surface and Coatings Technology*, **142-144**, 861-867, (2001).

[5] C.-H. Ma, J.-H. Huang and H. Chen, *Thin Solid Films*, **418**, 73-78, (2002).

[6] S. Bein, C. L. Calvez and J. Lebrun, *Z. Metallkd.*, **89**, 289-296, (1998).

[7] J. A. Thornton and D. W. Hoffman, *Thin Solid Films*, **171**, 5-31, (1989).

[8] K. Tanaka, T. Ito, Y. Akiniwa and T. Ishii, J. Soc. Mater. Sci. Japan, **52**, 738-743, (2003).

[9] S. Tsuchiya, T. Oshika, S. Agawa, M. Sato and I. Hirosawa, SPring-8 User Experiment Report, **11**. to be published.

[10] S. Tsuchiya, T. Oshika, S. Agawa, M. Sato and I. Hirosawa, SPring-8 User Experiment Report, **10**, 105, (2003).

(Received October 10, 2003; Accepted March 31, 2004)